Neuron
Article

Olig1 Function Is Required to Repress *Dlx1/2* and Interneuron Production in Mammalian Brain

John C. Silbereis,[1,2,3,6] Hiroko Nobuta,[1,2,6] Hui-Hsin Tsai,[1,2,6] Vivi M. Heine,[1,2,8] Gabriel L. McKinsey,[3,4] Dimphna H. Meijer,[5] MacKenzie A. Howard,[2] Magda A. Petryniak,[1,7] Gregory B. Potter,[1,7] John A. Alberta,[5] Scott C. Baraban,[2] Charles D. Stiles,[5] John L.R. Rubenstein,[4] and David H. Rowitch[1,2,6,*]
[1]Department of Pediatrics, Eli and Edythe Broad Institute for Stem Cell Research and Regeneration Medicine
[2]Department of Neurosurgery
[3]Neuroscience Graduate Program
[4]Department of Psychiatry
University of California, San Francisco, San Francisco, CA 94143, USA
[5]Department of Cancer Biology, Dana-Farber Cancer Institute, Boston, MA 02115, USA
[6]Howard Hughes Medical Institute, Chevy Chase, MD 20815, USA
[7]Present address: Department of Pediatrics, Oregon Health & Science University, P.O. Box 574Mail Code L481, Portland, OR 97239
[8]Present address: Department of Child Neurology, Center for Neurogenomics and Cognitive Research, VU University Medical Center, Amsterdam, NL
*Correspondence: rowitchd@peds.ucsf.edu
http://dx.doi.org/10.1016/j.neuron.2013.11.024

SUMMARY

Abnormal GABAergic interneuron density, and imbalance of excitatory versus inhibitory tone, is thought to result in epilepsy, neurodevelopmental disorders, and psychiatric disease. Recent studies indicate that interneuron cortical density is determined primarily by the size of the precursor pool in the embryonic telencephalon. However, factors essential for regulating interneuron allocation from telencephalic multipotent precursors are poorly understood. Here we report that *Olig1* represses production of GABAergic interneurons throughout the mouse brain. *Olig1* deletion in mutant mice results in ectopic expression and upregulation of *Dlx1/2* genes in the ventral medial ganglionic eminences and adjacent regions of the septum, resulting in an ~30% increase in adult cortical interneuron numbers. We show that Olig1 directly represses the *Dlx1/2 I12b* intergenic enhancer and that *Dlx1/2* functions genetically downstream of *Olig1*. These findings establish *Olig1* as an essential repressor of *Dlx1/2* and interneuron production in developing mammalian brain.

INTRODUCTION

The balance between excitatory and inhibitory tone in the cerebral cortex is mediated largely by relative activity of excitatory glutamatergic pyramidal cells and inhibitory γ-aminobutyric acid-containing (GABAergic) local circuit neurons, also known as interneurons (INs). GABAergic INs regulate sensory fields, plasticity, and the frequency and tone of cortical oscillatory activity (Alonso and Swadlow, 2005; Kehrer et al., 2008; Lehmann et al., 2012; Lewis et al., 2005; Llinás et al., 2005; Schiller and Tehovnik, 2005). Disruption of excitatory/inhibitory balance is linked to epilepsy, neurodevelopmental, and psychiatric disorders (Ben-Ari, 2006; Cobos et al., 2005; Corbin et al., 2001; Han et al., 2012; Hashimoto et al., 2003, 2008; Kehrer et al., 2008; Rossignol, 2011; Rubenstein, 2010; Rubenstein and Merzenich, 2003; Yizhar et al., 2011).

A recent study suggests that the size of the cortical IN population is determined primarily in the early embryo at time of specification, rather than by neurotrophic competition, and programmed cell death later in development (Southwell et al., 2012). Transplanted IN precursors are capable of functional integration into the adult brain (Alvarez-Dolado et al., 2006; Southwell et al., 2010) and can attenuate seizures in rodent models of epilepsy (Baraban et al., 2009; Hunt et al., 2013). Increased IN population size also induces and extends critical periods for ocular dominance plasticity (Southwell et al., 2010). Thus, generating the appropriate number of cortical neurons during development is crucial. However, the factors that normally limit the size of the IN progenitor pool are poorly understood and essential repressors of IN developmental programs have not been described.

Specification of cortical inhibitory neurons from multipotent precursors in the embryonic brain is complex, involving the following: (1) patterning of spatially discrete progenitor pools for specific subtypes, (2) temporal regulation of multiphase neurogenesis, and (3) mechanisms of neuron versus oligodendroglial (OL) cell fate acquisition (Butt et al., 2005; Kessaris et al., 2006; Marín, 2012; Wonders et al., 2008). Cortical inhibitory neurons are produced from E10 to E17 in the medial ganglionic eminence (MGE), anterior entopeduncular area (AEP; a ventral region of the MGE), caudal ganglionic eminence (CGE), and preoptic areas (POA) of the ventral telencephalon; they then migrate tangentially into the cerebral cortex (Anderson et al., 1997; Corbin et al., 2001; Miyoshi et al., 2007; Wonders and Anderson, 2006). Parvalbumin (PV) and calretinin (CR) positive cells are derived relatively late in embryogenesis from

progenitor domains that produce both OLs and INs, whereas neuropeptide-Y (NPY) and somatostatin (SST) subtypes are born prior to the onset of OL specification (Kessaris et al., 2006; Miyoshi et al., 2007; Taniguchi et al., 2013; Wonders et al., 2008). In contrast, the adjacent regions of the lateral ganglionic eminence and the telencephalic septum generate neurons of the ventral forebrain and olfactory bulb (OB) but are not thought to give rise to cortical INs (He et al., 2001; Kessaris et al., 2006; Petryniak et al., 2007; Rubin et al., 2010). *Dlx1/2* function is necessary for the establishment of IN cell production within these regions and differentiation into GABAergic INs (Anderson et al., 1997). Though the mechanisms that control OL versus IN fate are poorly understood, we have shown that *Dlx1/2* function is required in the MGE and AEP to control the neuron-glial switch, promoting neurogenesis at the expense of OLs through repression of *Olig2* (Petryniak et al., 2007). In contrast, *Olig2*-null animals show no abnormalities in early IN development (Petryniak et al., 2007; Furusho et al., 2006; Ono et al., 2008).

Olig1 is expressed in the embryonic neuroepithelium of the ventral forebrain (Petryniak et al., 2007), which can give rise to INs and OLs (Mukhopadhyay et al., 2009; Samanta et al., 2007). However, *Olig1* function is generally thought to be limited to late stages of OL development to promote differentiation (Lu et al., 2002; Xin et al., 2005) and remyelination (Arnett et al., 2004). Here, we show a surprising role for *Olig1* as an upstream repressor of *Dlx1/2* and GABAergic IN production in the embryonic brain, establishing that *Olig1* functions in the regulation of the neuron-glial switch. Loss of *Olig1* derepresses production of late CR and PV IN subtypes in ventral MGE, AEP, and regions of the MGE connected to the septum, resulting in a 30% excess of INs in adult cortex. Postnatally, *Olig1*-null neural progenitors produced excessive numbers of INs and are deficient in OL production. We show Olig1 directly binds and represses the *I12b* enhancer element, a known *Dlx1/2* intergenic *cis*-acting DNA regulatory sequence, and using a newly generated floxed conditional *Dlx1/2* knockout allele, we show that *Dlx1/2* lies genetically downstream of *Olig1*. Together, these findings demonstrate that *Olig1* is an essential repressor of GABAergic neuron production in the mammalian brain.

RESULTS

Inhibitory IN Numbers Are Increased in the Cortex of *Olig1*-Null Animals

To assess *Olig1*-dependent regulation of IN production, we first analyzed IN markers in the adult (P50) motor and somatosensory cortex of *Olig1*-null and control animals by immunohistochemistry (IHC) (Figure 1A). Evaluation of IN subtypes in motor and somatosensory cortex demonstrated that there was an approximate 35% increase in PV+ and CR+ IN subtypes, but not SST+ or NPY+ subtypes (Figures 1B, 1I–1K, and 1M). We also observed an ~30% increase in cells expressing the pan-IN lineage markers GABA and GAD67 (Figures 1G and 1H; Figures S1K and S1L available online). We next determined if the laminar distribution of INs was abnormal. Increased numbers of PV+ and CR+ INs were present throughout the cortical layers. We did not find any difference in the laminar distribution of SST+ and NPY+ cells (Figures 1N–1Q). SST+ and NPY+ neurons are generated early in telencephalic neurogenesis before E13. In contrast, CR+ neurons are generated at later stages and the PV+ subtype is generated throughout embryogenesis, coinciding with the onset of OL specification (Kessaris et al., 2006; Miyoshi et al., 2007; Taniguchi et al., 2013; Wonders et al., 2008). Thus, *Olig1* acts to limit late-born INs generated simultaneously with OLs, but not early-born INs. Normal numbers of glutamatergic and cholinergic neurons were observed in *Olig1*-null animals (data not shown).

To confirm our findings, we conducted unbiased stereological analysis of the number of GAD67+ cells throughout the cortex and determined that the density and estimated total number of GAD67+ cells was increased by ~25% throughout the cortex (Figures S1K–S1L). Cortical volume was unchanged in *Olig1*-null mice (Figures 1B and S1M). To ensure that our results are not due to misexpression of IN markers with other cell types, we performed IHC for PV and GAD67 with markers of pyramidal cells (Tbr1), OLs (Olig2), microglia (Iba1), and astrocytes (GFAP). As shown (Figures S1G–S1J), we found no instance of abnormal IN marker expression in *Olig1*$^{-/-}$ brains.

Inhibitory PV+ INs synapse on the soma of cortical pyramidal cells, whereas CR+ neurons synapse mainly on the soma of other INs (Caputi et al., 2009; Freund and Buzsáki, 1996; Gonchar and Burkhalter, 1999). In keeping with the counts described above, we found an ~30% increase of PV+ puncta on the soma of layer 2/3 and 5/6 pyramidal neurons of somatosensory and motor cortex (Figures 1C and 1D). Moreover, such puncta also expressed vesicular GABA transporter (VGAT) (Figure 1E), a marker of inhibitory synapses (Bragina et al., 2007). Quantification of VGAT+ puncta in dendritic fields revealed no differences in the number of inhibitory synapses on dendrites, consistent with our finding that SST+ cell numbers are not affected in *Olig1*$^{-/-}$ mice (Figures 1E and 1F).

Increased IN Number Does Not Alter Inhibitory Events on Cortical Pyramidal Cells: Evidence of Postsynaptic Gephyrin-Mediated Compensation

There are a myriad of cell-intrinsic and synaptic homeostatic mechanisms that control inhibition in cortical circuits (Pozo and Goda, 2010; Turrigiano, 2011). *Olig1*$^{-/-}$ mice provided a unique system to determine if increases in endogenously derived INs are sufficient to enhance inhibition in the adult cortex. To test this possibility, we performed voltage-clamp analysis of inhibitory postsynaptic currents in layer 5 pyramidal cells in acute cortical slices derived from P35 mice. As a functional measure of inhibitory tone, we analyzed both spontaneous and miniature inhibitory postsynaptic potentials (sIPSPs and mIPSPs). We found no significant increase in inhibitory activity onto pyramidal cells in terms of event frequency, amplitude, or kinetics (Figures S2A and S2B; data not shown). Because we observed more presynaptic VGAT puncta, expressed at the soma of cortical neurons, we hypothesized that a postsynaptic compensatory mechanism might regulate inhibition in *Olig1*$^{-/-}$ mice. Gephyrin, a scaffolding protein that regulates recruitment, stability, and clustering of GABA receptors at the postsynapse, is downregulated in response to increased

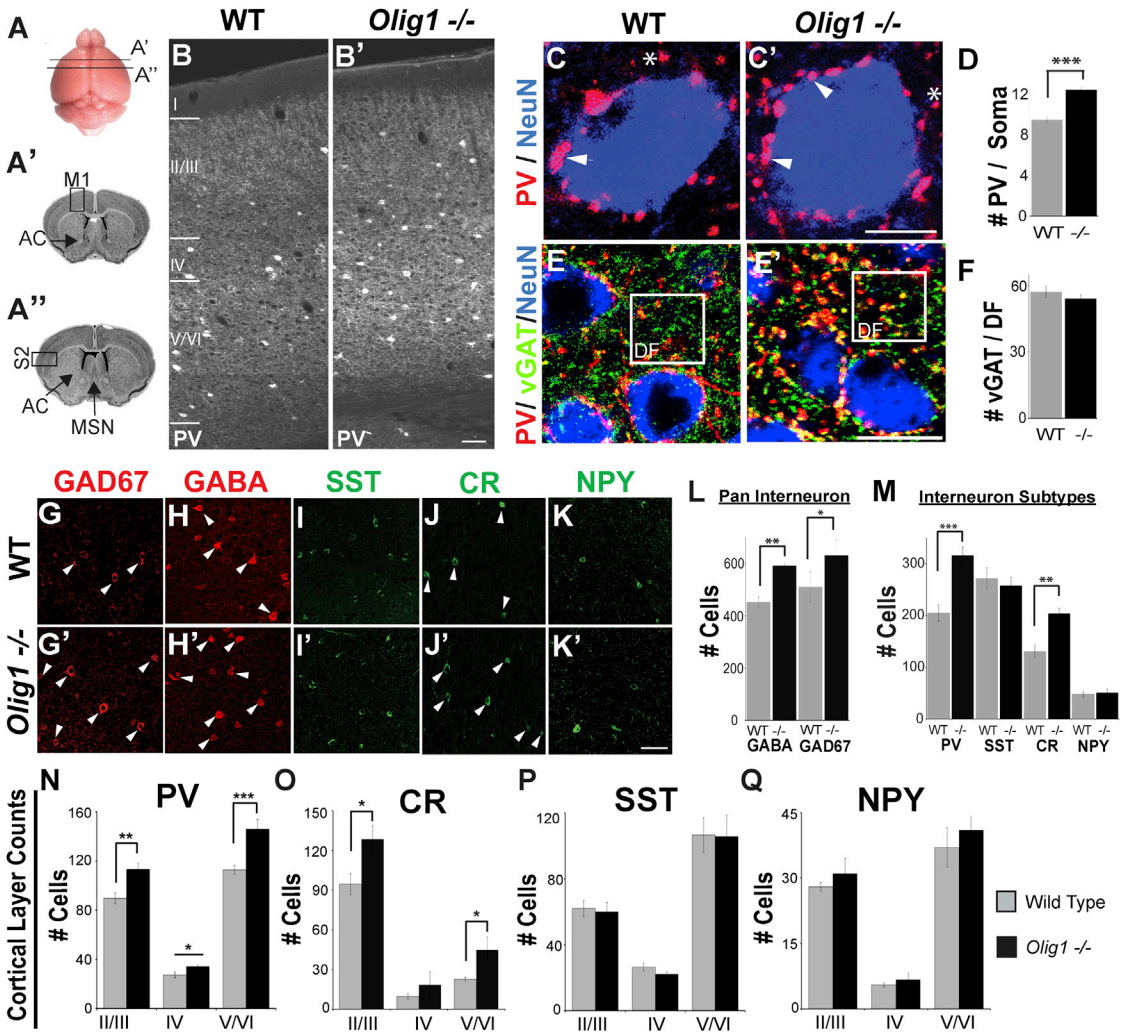

Figure 1. Increase in Interneuron Numbers in the Cerebral Cortex of Adult *Olig1*-Null Mutant Mice

(A) Representation of regions of secondary somatosensory cortex (S2) and primary motor cortex (M1) in which INs were quantified.

(B) Representative images of parvalbumin (PV) in wild-type (WT) versus *Olig1*-null (*Olig1*$^{-/-}$) motor cortex. Note the increased number of PV+ cell bodies.

(C) Representative image showing increases in PV+ (red) synaptic puncta localized to NeuN+ (blue) soma in *Olig1*$^{-/-}$ versus WT M1. Arrowheads point to soma localized PV+ puncta; asterisks denote non-soma-localized puncta.

(D) Quantification of PV+ synaptic puncta colocalizing NeuN-positive soma in M1.

(E) Representative image showing VGAT (green), PV (red), and NeuN (blue). As shown in the boxed region, VGAT+ (green)/PV− (red) synaptic puncta in dendritic fields (DF) are identical in *Olig1*$^{-/-}$ versus WT M1. Note that PV+ (red) puncta colocalize VGAT confirming they label GABAergic synapses.

(F) Quantification of the number of VGAT+ puncta in dendritic fields demonstrating that there is not a significant increase in the number of VGAT+ neuronal synapses in dendritic fields of *Olig1*$^{-/-}$ cortex versus WT.

(G–K) Representative images of INs in *Olig1*$^{-/-}$ and wild-type cortex. Arrows point to cell bodies of cell types for which significant differences were observed.

(G and H) Two micrometer confocal projections of pan IN markers GAD67 (G) and GABA (H).

(I–K) Two micrometer confocal projections of IN subtype markers somatostatin (SST) (I), calretinin (CR) (J), and neuropeptide-Y (NPY) (K).

(L and M) Quantification of the number of cells expressing the pan IN markers (L) and IN subtypes (M). Cell counts were taken from micrographs of S2 and M1 in two anterior-to-posterior serial coronal sections as shown in (A).

(N–Q) Quantification of the number of cells expressing IN subtypes within distinct lamina of the cortex (II/III, IV, and V/VI) as demonstrated in (B). Cell counts were taken from micrographs of S2 and primary M1 (For all quantifications, mean ±SEM; n = 3–4; *p < 0.05, **p < 0.01, ***p < 0.005; two-tailed unpaired Student's t test). In (B'), (E'), and (K''), scale bar indicates 50 μm; in (C') and (K''), scale bars indicate 5 μm, and in (E'), scale bar indicates 15 μm. For abbreviations, AC indicates anterior commissure, DF indicates dendritic field, IN indicates interneuron, M1 indicates primary motor cortex, MSN indicates medial septal nucleus, and S2 indicates secondary somatosensory cortex. See also Figures S1 and S2.

GABAergic activity (Poulopoulos et al., 2009; Prior et al., 1992; Saiepour et al., 2010; Tretter et al., 2008, 2012). As demonstrated (Figure S2C), we observed normal numbers of gephyrin puncta identified by IHC at the postsynapse. We also noted that some CR+ INs make inhibitory connections with other INs, and thus, excess CR+ INs may also limit the activity of other IN subtypes

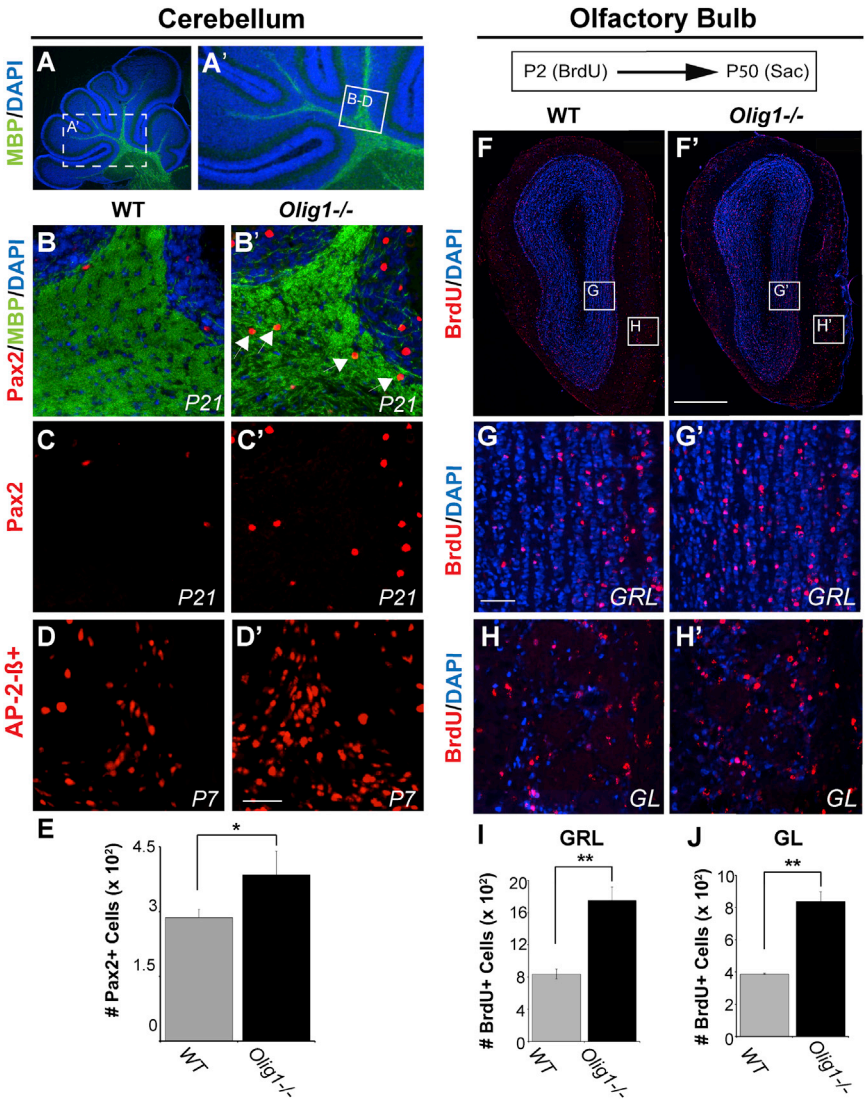

Figure 2. Increase in the Number of Interneurons in *Olig1*$^{-/-}$ Cerebellum and Olfactory Bulb

(A) Low magnification image of MBP (green) and DAPI (blue) of juvenile cerebellum. The box represents the region where the images in (B)–(D) were taken.

(B) Image taken of P21 cerebellum showing Pax2+ INs (red) and anatomy of cerebellar lobules with white matter defined by dense MBP immunoreactivity (green) and the granule layer defined by dense DAPI staining (blue). Note the ectopic presence of Pax2+ INs in the white matter (arrows) in the *Olig1*$^{-/-}$ mice.

(C) Single-channel image of Pax2 (red) staining in panel a demonstrating increased numbers of Pax2+ INs in *Olig1*$^{-/-}$ mice.

(D) Representative images of IHC showing increased numbers of cerebellar IN precursor cells expressing AP-2β in *Olig1*$^{-/-}$ versus WT mice at P7.

(E) Quantification of Pax2+ cells in the P21 cerebellum demonstrating a statistically significant increase in Pax2+ cells *Olig1*$^{-/-}$ versus WT mice.

(F) Low-magnification image of the olfactory bulbs of WT (F) versus *Olig1*$^{-/-}$ (F') mice injected with BrdU at P2 stained for BrdU (red) and DAPI (blue).

(G) Higher-magnification images of the granule cell layer corresponding to the box insets labeled (G) and (G') in (F).

(H) Higher-magnification images of the glomerular layer corresponding to the box inset labeled (H) and (H') in panel (F).

(I and J) Quantification of the number of BrdU+ cells in the P50 granule cell layer (GRL) and glomerular layer (GL), respectively, following BrdU injection at P2, demonstrating a statistically significant increase in BrdU+ cells in *Olig1*$^{-/-}$ versus WT mice following BrdU injection at P2. In (C'), scale bar indicates 50 μm; in (F), scale bar indicates 500 μm; and in (G), scale bar indicates 50 μm. (For all quantifications, mean ±SEM; n = 3; *p < 0.05, **p < 0.01, two-tailed unpaired Student's t test.) For abbreviations, GRL indicates granule layer and GL indicates glomerular layer. See also Figure S1.

in *Olig1* $^{-/-}$ mice (Caputi et al., 2009; Freund and Buzsáki, 1996; Gonchar and Burkhalter, 1999).

Olig1 Represses Neurogenesis in the Cerebellum and OB

We next assessed *Olig1* function in the cerebellum (CB) and OB, brain areas that exhibit protracted neurogenesis (Maricich and Herrup, 1999; Schüller et al., 2006). As shown (Figures 2A–2C and 2D), we observed an ~30% surplus of AP2Beta+ and Pax2+ cerebellar INs at P7 and P21, respectively. Robust neurogenesis and neural cell turnover persists in the OB throughout life and is regulated by Dlx1/2 (Alvarez-Buylla et al., 2002; Long et al., 2007). To assess neurogenesis in the OB, we conducted birth dating assays by injecting the thymidine analog Bromodeoxyuridine (BrdU) intraperitoneally into P2 pups and analyzing OBs in tissue harvested by perfusion at P50. These mice exhibited approximately 2-fold increases in the numbers of BrdU+ cells in the granule layer and glomerular layer (Figures 2F–2J). In summary, these findings provide evidence that *Olig1* has a general role in repressing IN production, including in the neocortex (PV+ and CR+ subtypes), CB (Pax2+ / AP2Beta+), and perinatal OB.

Olig1$^{-/-}$ Mice Produce Fewer Numbers of Oligodendrocytes

Given previous evidence for common precursor domains for INs and OLs in the embryonic telencephalon, perinatal CB, and OB throughout life (Goldman et al., 1997; Menn et al., 2006; Petryniak et al., 2007; Silbereis et al., 2009; Zhang and Goldman, 1996), we assessed the impact of *Olig1* loss of function on the OL population in the adult cerebral cortex and CB by histological analysis. The numbers of cells expressing the pan-OL marker Olig2, as well as the mature OL markers *PLP* and APC, are all reduced in the corpus callosum, motor cortex, and cerebellar white matter of the P21 and P50 mouse brain (Figures S1A–S1F).

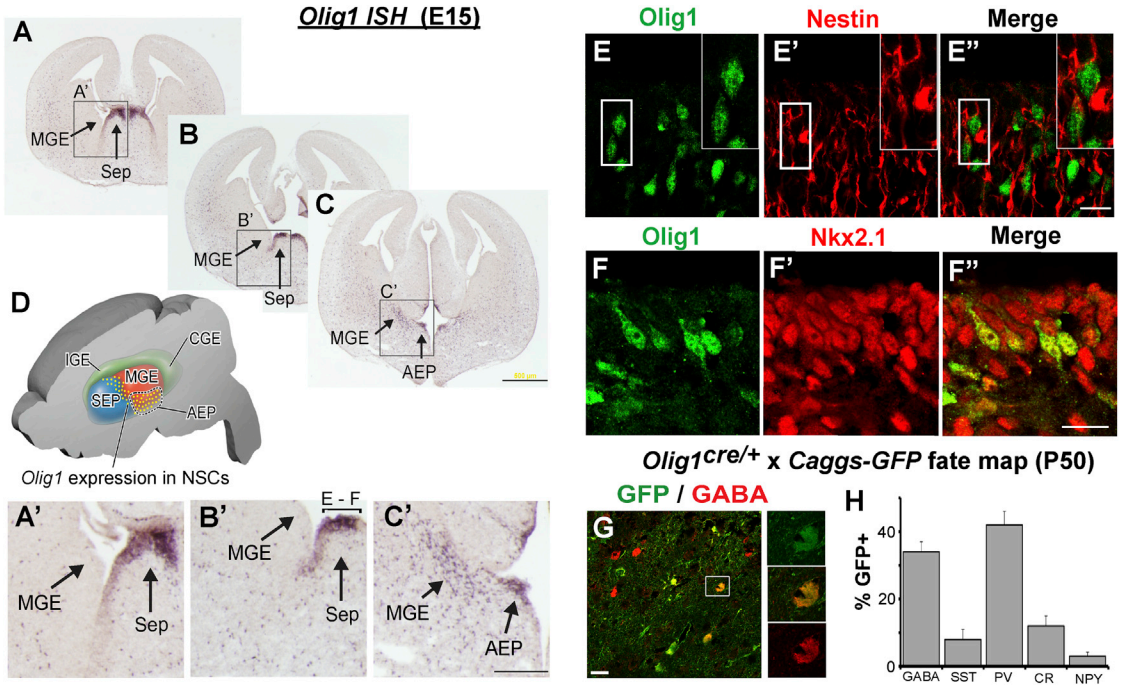

Figure 3. *Olig1* Is Expressed in Ventral Telencephalic Progenitors for Interneurons

(A–C) Anterior-to-posterior serial sections of in situ hybridization for *Olig1* demonstrating expression in the ventricular zone (VZ) of dorsal embryonic septum (sep), ventral medial ganglionic eminence (vMGE), and anterior enteropeduncular area (AEP).

(D) A cartoon of the domain in which *Olig1* is expressed in the ventricular zone. (Da')–(Dc') Higher magnification view of the regions expressing *Olig1*. These regions are denoted by the boxes and arrows in (A)–(C). The bracket labeled "e–f" in image Db' defines the regions shown in (E) and (F).

(E) Confocal projections showing that Olig1 (green, [E]) colocalizes the radial glia protein Nestin (red, [E']; merged image, [E"]).

(F) Confocal projections showing that Olig1 (green, [F]) colocalizes Nkx2.1+ progenitors (red, f'; merged image [F"]) which are known to give rise to both INs and OLs.

(G) Representative image of fate mapping in cerebral cortex from *Olig1*$^{cre/+}$ mice crossed to the *Caggs-Gfp* reporter mouse, showing ~35% of GABA+ INs (red) are derived from *Olig1*+ progenitors as defined by the expression of the GFP+ (green) reporter protein.

(H) Quantification of the proportion of a panel of IN markers (GABA, PV, SST, CR, or NPY) colabeling GFP (percentage ±SEM). Note the preferential labeling of PV+ subtypes. In (C), scale bar indicates 500 μm; in (Cc'), scale bar indicates 200 μm; in (E") and (F"), scale bar indicates 20 μm. Additional abbreviations are as follows: lge, indicating lateral ganglionic eminence, and cge, indicating caudal ganglionic eminence.

Olig1 Is Expressed in Multipotent Telencephalic Progenitors that Produce Cortical IN

GABAergic INs of somatosensory and motor cortex develop from the ventral embryonic telencephalon under control of *Dlx1/2* and other transcriptional programs (Anderson et al., 1997; Wonders and Anderson, 2006). As shown (Figures 3A–3D), we detected *Olig1* mRNA transcripts in the AEP and ventral MGE telencephalic regions that express *Dlx1/2* (Petryniak et al., 2007), as well as caudal/dorsal regions of embryonic septum, which produces OLs but is not thought to produce cortical INs (Rubin et al., 2010). *Nkx2.1* is a hedgehog-responsive gene critical for establishing progenitors of ventral identity that derive both forebrain OLs and INs (Butt et al., 2008; Elias et al., 2008; Kessaris et al., 2006; Maricich and Herrup, 1999). As shown (Figures 3E and 3F), we found that Olig1+ cells colabeled with Nestin and Nkx2.1.

A second line of evidence assigning *Olig1* expression to IN progenitors was provided by fate mapping with *Olig1*-cre. Our analysis in the adult (P50) neocortex, consistent with previous studies (Mukhopadhyay et al., 2009; Samanta et al., 2007), showed that *Olig1-cre* precursors fate mapped to ~35% of GABAergic cells and ~45% of PV+ INs, but fewer INs of other subtypes. In contrast, we found no labeling of glutamatergic cortical neurons (Figures 3G and 3H; data not shown). Together, these findings indicate *Olig1* is expressed in multipotent precursor cells for GABAergic INs, particularly the PV+ subtype.

Olig1 Represses Telencephalic IN Genetic Programs

We next used in situ hybridization (ISH) to assess expression of *Lhx6*, *Dlx1*, and *Dlx2*, genes necessary for the genesis of INs from MGE, AEP, CGE, and preoptic area (POA) of wild-type and *Olig1*$^{-/-}$ E15 embryonic brain. *Olig1* mutants showed expansion of *Lhx6*, *Dlx1*, and *Dlx2* expression into the ventral MGE, the AEP, and the caudal septum (Figures 4A–4H). To quantify this upregulation and assess the expression of *Vax1* and *Sp8* (two additional genes associated with IN production in the telencephalon), we dissected the caudal septum, AEP, and ventral MGE from wild-type and *Olig1*-null embryos and performed qPCR (Anderson et al., 1997; Taglialatela et al., 2004; Waclaw et al., 2006). We observed 2-fold to 4-fold increased

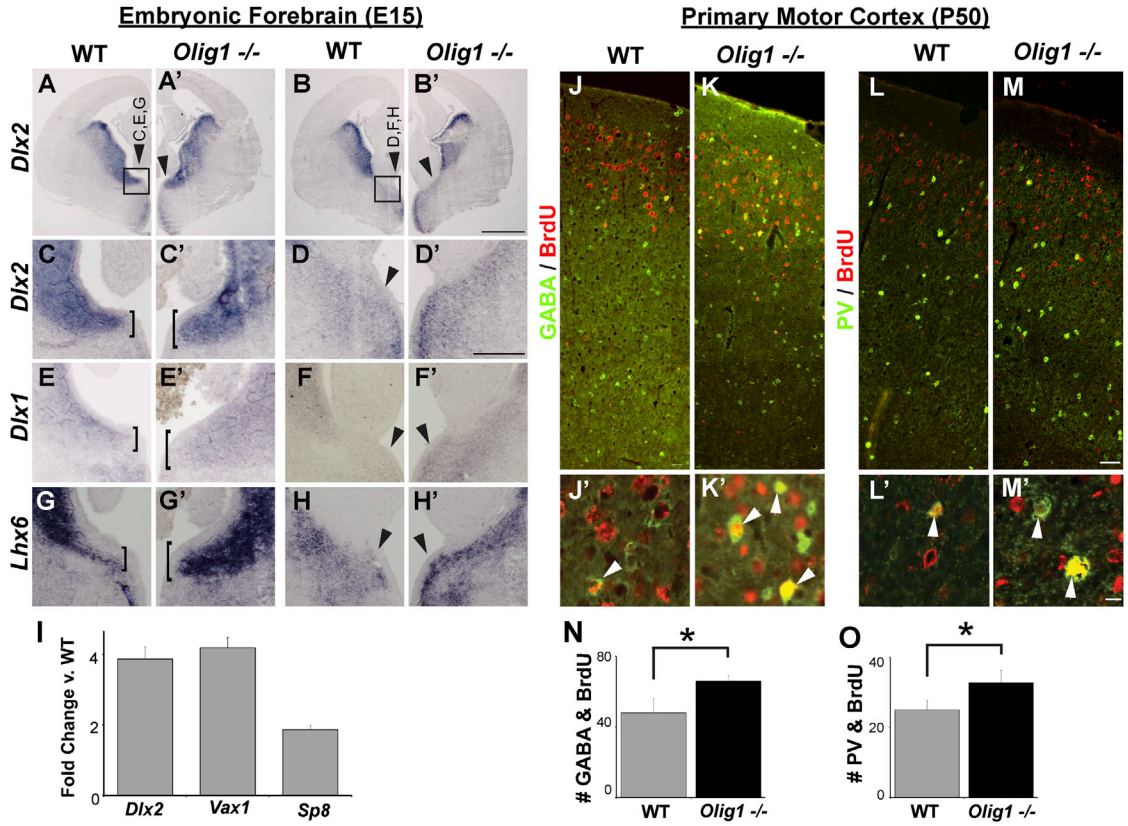

Figure 4. *Olig1* Represses Prointerneuron Genetic Programs in Embryonic Brain

(A and B) Representative images of in situ hybridization for *Dlx2* in two anterior to posterior sections of E15.5 forebrain showing upregulation of *Dlx2* in the AEP and ventral MGE ([A'] and [B'], respectively) denoted by the box and arrowheads, respectively.

(C and D) High-magnification of *Dlx2* expression delineated in the boxed regions of (A) and (B). The brackets in (C) emphasize the expansion of the domain expressing *Dlx2* in the AEP, and the arrowheads denote increased expression in ventral MGE.

(E–H) High-magnification images showing similar upregulated expression of (E and F) *Dlx1* and (G and H) the proneural gene *Lhx6*.

(I) Graph showing quantitative PCR results of cDNA samples derived from RNA samples taken from the E15 ventral forebrain of *Olig1*-null and WT mice. Note upregulation of the proneural genes *Dlx2*, *Vax1*, and *Sp8*.

(J and K) Representative images of GABA (green) and BrdU (red) birth dating analysis in P50 cortex demonstrating that more GABA+ INs are labeled by BrdU injected at E16. Higher-magnification images demonstrating colabeling are shown in (J') and (K').

(L and M) Representative images of PV (green) and BrdU (red) birth dating analysis in P50 cortex demonstrating that more PV+ INs are labeled by BrdU injected at E16. Higher-magnification images demonstrating colabeling are shown in (L') and (M').

(N and O) Quantification of GABA+ (n) or PV+(o) cells colocalizing BrdU. BrdU was injected at E16. (Mean ±SEM; n = 3; *$p < 0.05$, two-tailed unpaired student's t test.) In (B'), scale bar indicates 500 μm; in (D'), scale bar indicates 200 μm; and (M) and (M'), scale bar indicates 50 μm. See also Figures S3, S4, and S5.

expression of *Dlx2*, *Vax1*, and *Sp8* (Figure 4I). These data indicate that loss of *Olig1* function results in upregulated expression of key transcription factors that drive IN cell fate acquisition.

Previously, gain-of-function studies have shown that Olig1 promotes OL specification from neural progenitors (Kim et al., 2011; Lu et al., 2000, 2001; Maire et al., 2010). To assess potential changes in embryonic OPC production, we assessed *PDGFRa*+ cells by ISH and quantified Sox10+ OPCs by IHC in *Olig1*$^{-/-}$ mutant and wild-type E15 embryos in the mantle of the ventral telencephalon. This showed a reduction in OPC number (Figures S3A–S3C). In contrast, we observed no significant change in levels of the mitotic cell marker phospho-histone H3 (PH3) in the septum, MGE, and AEP (Figures S3D–S3F). Together, these findings suggest that *Olig1* function is required to promote OPC production at the expense of INs in the ventral telencephalon, but it does not regulate IN precursor proliferation. Further, this shows a unique function of *Olig1* as a repressor of IN development, because *Olig2*-null mice, which lack OPCs, show normal expression of *Dlx2* (Petryniak et al., 2007) and IN precursor numbers identified by expression of GAD67 mRNA in the ventral telencephalon (Figure S4) (Furusho et al., 2006; Ono et al., 2008).

To confirm the birthdate of ectopic cortical INs in the *Olig1* mutant embryonic forebrain, we injected bromodeoxyuridine (BrdU) into pregnant dams at E16. BrdU colabeling analyses with PV and GABA revealed an approximately 30% increase in the number of INs generated at these ages (Figures 4J–4O). Interestingly, at P0 we observed enhanced expression of *Dlx2* in the subventricular zone (SVZ) of *Olig1*-null animals (Figures S5A–S5D), raising the possibility of persistent IN production.

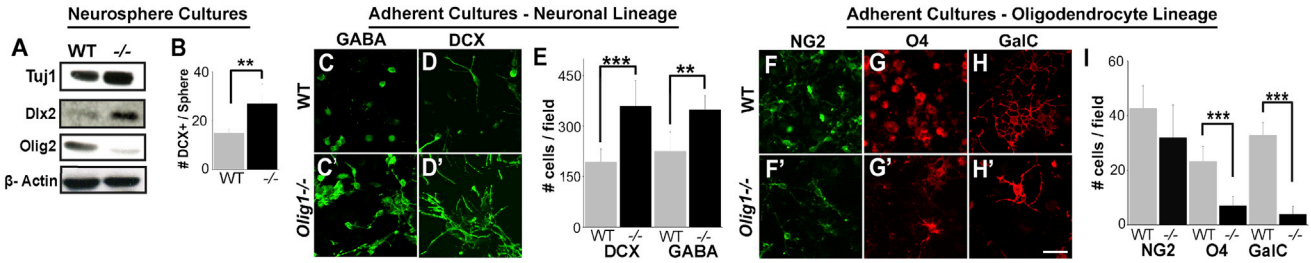

Figure 5. *Olig1* Regulates Interneuron versus Oligodendrocyte Cell Fate in Neural Stem Cell Cultures

(A) Western blots from WT and *Olig1*$^{-/-}$ neurospheres for the neuronal protein Tuj1, Dlx2, and Olig2 showing increased expression of neuronal proteins and decreased expression of Olig2.

(B–D) Quantification of number of DCX+ cells per neurosphere identified by IHC (C and D). Representative images of neural progenitor monolayer cultures derived from P3 WT and *Olig1*$^{-/-}$ SVZ, differentiated for 1 week and stained for DCX (C) and GABA (D).

(E) Quantification of the number of DCX and GABA cells captured at three defined coordinates in chamber slide wells reveals increased numbers of DCX and GABA+ cells in *Olig1*$^{-/-}$ versus wild-type.

(F–H) Representative images of neural progenitor monolayer cultures derived from P3 WT and *Olig1*$^{-/-}$ SVZ, differentiated for 1 week and stained for NG2 (G), O4 (H), and GalC.

(H) Scale bar indicates 50 μm. See also Figure S5.

(I) Quantification of the number of NG2, O4, and GalC cells captured at three defined coordinates in chamber slide wells reveals decreased numbers of O4 and GalC+ cells in *Olig1*$^{-/-}$ versus wild-type. (For all quantifications, mean ±SEM; n = 3 experiments, four slide wells per experiment; *p < 0.05; **p < 0.01; ***p < 0.005; two-tailed unpaired Student's t test).

However, BrdU birth dating at P2 ruled this out (Figures S5E and S5F). Together, these findings indicate that *Olig1* regulates neuron-glial fate choice in the embryonic telencephalon.

Postnatal Roles for *Olig1* in Suppression of IN Production

The finding of increased OB neurogenesis perinatally and ectopic *Dlx2* expression in *Olig1*-null dorsal SVZ at P0 suggested there may be persistent roles for *Olig1* in neural stem cells (NSCs). To test if *Olig1* regulates cell fate in defined culture conditions, we harvested progenitors from P3 anterior SVZ and then cultured progenitor cells as neurospheres or adherent monolayers of NSCs. Neurospheres were expanded in EGF and FGF and then transferred to factor-free medium overnight to induce differentiation markers. Western blot analysis of total proteins demonstrated increased levels of neuron-specific Tuj1 and Dlx2 expression in *Olig1*-null neurospheres compared to wild-type; in contrast, Olig2 levels were dramatically reduced (Figure 5A). In keeping with these findings, *Olig1*-null spheres showed enhanced capacity to produce young doublecortin (DCX)+ neurons (Figure 5B). As shown (Figures 5C–5E), *Olig1* loss of function enhanced GABAergic IN production from NSC monolayer cultures. By contrast, monolayers derived from *Olig1*-null progenitors were deficient in production of NG2+, O4+, and GalC+ OL lineage cells (Figures 5F–5I), which respectively label OPCs, premyelinating OLs, and myelinating OLs. GFAP+ astroglial production was unaffected (data not shown). Thus, *Olig1* function is required in cultured postnatal neural progenitors to repress IN production and preserve oligodendrogenesis.

Evidence that Olig1 Is a Direct Repressor of the *Dlx1/2 I12b* Intergenic Enhancer

Olig1 acts as a transcriptional repressor (Lee et al., 2005; Novitch et al., 2001; Sun et al., 2003). Thus, we hypothesized that *Olig1* might directly repress *Dlx1* and/or *Dlx2*, which colocalize within 10 kb of each other on mouse chromosome 2. This potential hierarchy is consistent with the observations that (1) *Olig1-cre* fate mapping labels 30% of cortical GABAergic neurons, (2) Olig1 protein shows segregated expression from Dlx2 in ventral telencephalon (Figure 6a), and (3) the previous finding that *Dlx1/2-cre* fate mapping fails to label Olig1-positive cells (Potter et al., 2009).

We tested whether *Olig1* might regulate *cis*-acting DNA regulatory sequences in the intergenic region of *Dlx1/2*. Activity of the *I12b* enhancer drives expression of *Dlx1/2* in the embryonic ventral telencephalon (Ghanem et al., 2007; Park et al., 2004; Poitras et al., 2007). We determined that the *I12b* enhancer contains three E-box sites, the canonical binding sequences for bHLH transcription factors including *Olig1* (Figures 6B, S6A, and S6B). We then used electrophoretic mobility shift assays (EMSA) to test *Olig1* binding to *Dlx1/2 I12b* E-box sites in vitro. As shown in Figures 6C and 6D, purified *Olig1* proteins shifted E-boxes 1 and 3, with the highest affinity for E-Box 1. Binding to E-box 1 was dose dependent and was abrogated by DNA mutation of E-box sites within the *I12b* enhancer (Figures 6C, 6D, and S6B). Specificity of *Olig1* binding was further tested by supershift assays, which demonstrated that treatment with an antibody against Olig1, but not with a control IgG antibody, inhibits binding of Olig1 protein to enhancer DNA sequences (Figures 6E and 6F).

To confirm that *Olig1* acts as a repressor of *Dlx1/2*, we next used a luciferase assay by cloning the *I12b* enhancer into the *pGL4* luciferase construct (Promega) and transfecting it into P19 cells. Because *Dlx1/2* are positive feedback regulators of their own expression via the *I12b* locus (Potter et al., 2009), we transfected a *Dlx2* expression construct to induce *I12b*-dependent luciferase activity. When an *Olig1* expression construct was transfected into these cells, it induced a nearly 3-fold reduction in luciferase activity (Figure 6G). Together, these

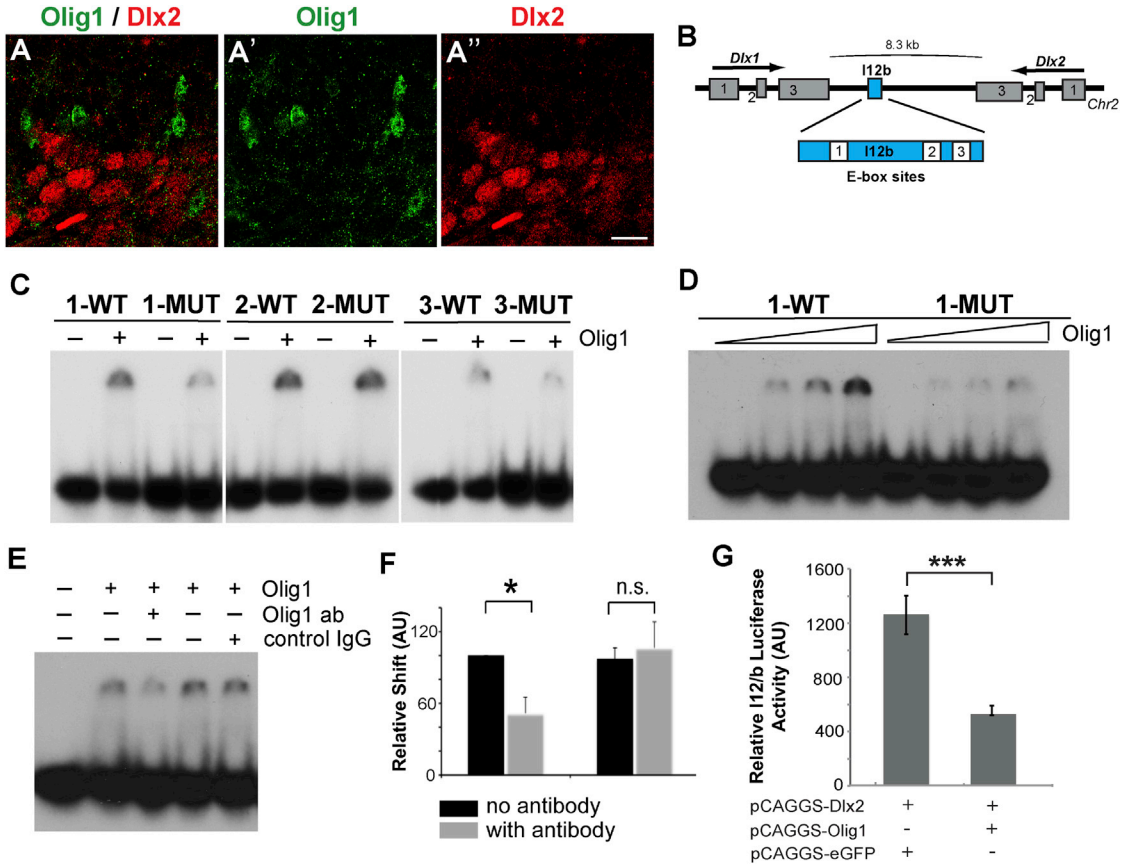

Figure 6. *Olig1* Is a Direct Repressor of *Dlx1/2* at the *I12B* Intergenic Enhancer

(A) One micrometer confocal projection demonstrating that Olig1 (green, [A']) and Dlx2 (red, [A"]) does not colocalize Olig1 in VZ.

(B) Schematic of the *Dlx1/2* bigenic region showing location of *I12B* intergenic enhancer and three E-box sites.

(C) Images of gels from electrophoretic mobility shift assays (EMSA) for the three *I12B* E-boxes (WT indicates wild-type and MUT indicates mutated) in presence or absence of *Olig1* protein. Note the strongest and most specific affinity for E-box site 1.

(D) Increasing concentrations of *Olig1* protein show dose-dependent affinity of *Olig1* for E-box 1 WT, but not for E-box 1 MUT.

(E) Supershift assay demonstrates that Olig1 antibody, but not control IgG antibody, inhibits binding of *Olig1* protein to E-box site 1.

(F and G) Quantification by densitometry of inhibition of DNA binding by incubation of Olig1 protein with Olig1 or control antibody (Student's t test; *$p < 0.05$).

(G) Luciferase assays demonstrate that Olig1 is a transcriptional repressor capable of reducing *Dlx2* induced *I12B* luciferase activity to 40% control levels (Student's t test; ***$p < 0.001$). In (A"), scale bar indicates 50 μm. See also Figures S5 and S6.

data provide biochemical evidence that *Olig1* functions upstream of *Dlx1/2* as a transcriptional repressor of the *Dlx1/2-I12b* enhancer.

Genetic Functions of *Dlx1/2* Downstream of *Olig1*

We next tested whether *Dlx1/2* function lies genetically downstream of *Olig1.* We generated a conditional floxed allele that removes *Dlx1* exons 2 and 3, the intergenic region, and *Dlx2* exons 2 and 3 upon exposure to cre recombinase (Figure 7A). Targeted ES cells produced chimeras that passed the allele through the germline (Figures 7B and 7C).

We first sought to determine whether the increase in cortical IN density in *Olig1*-null mice was *Dlx1/2*-dependent in vivo. To test specific requirements of *Dlx1/2* in the *Olig1* lineage, we crossed our *Olig1*-null *cre* knockin mice ($Olig1^{cre(KI)/cre(KI)}$), in which the *Olig1* coding sequence has been replaced with a cre recombinase gene (Lu et al., 2002), to the *Dlx1/2* floxed mice. Using these cre knockin mice, we were able to confine *Dlx* gene excision in *Olig1*-null animals to the *Olig1* expression domain. $Olig1^{cre(KI)/cre(KI)} \times Dlx1/2^{fl/fl}$ animals failed to thrive, typically died in the neonatal period, and never survived past P21, precluding analysis of PV populations in the adult cortex. However, $Olig1^{cre(KI)/cre(KI)} \times Dlx1/2^{fl/+}$ animals were viable into adulthood, at which point analysis of the cortices showed normalization of INs identified by IHC for GAD67 and PV (Figures 7D–7G and S7A–S7D).

To further establish *Dlx1/2* functions downstream of *Olig1*, we derived NSC monolayers from the ventral telencephalon of E14 $Olig1^{cre(KI)/cre(KI)} \times Dlx1/2^{fl/fl}$, $Olig1^{cre(KI)/cre(KI)} \times Dlx1/2^{+/+}$, and wild-type mice. As shown (Figures 7H–7I and 7K–7L), we observed that the increased IN production characteristic of $Olig1^{cre(KI)/cre(KI)}$ NSCs was normalized in $Olig1^{cre(KI)/cre(KI)} \times Dlx1/2^{fl/fl}$ NSCs. Conversely, we observed complete rescue of OL specification in $Olig1^{cre(KI)/cre(KI)}$; $Dlx1/2^{fl/fl}$ NSCs (Figures 7J

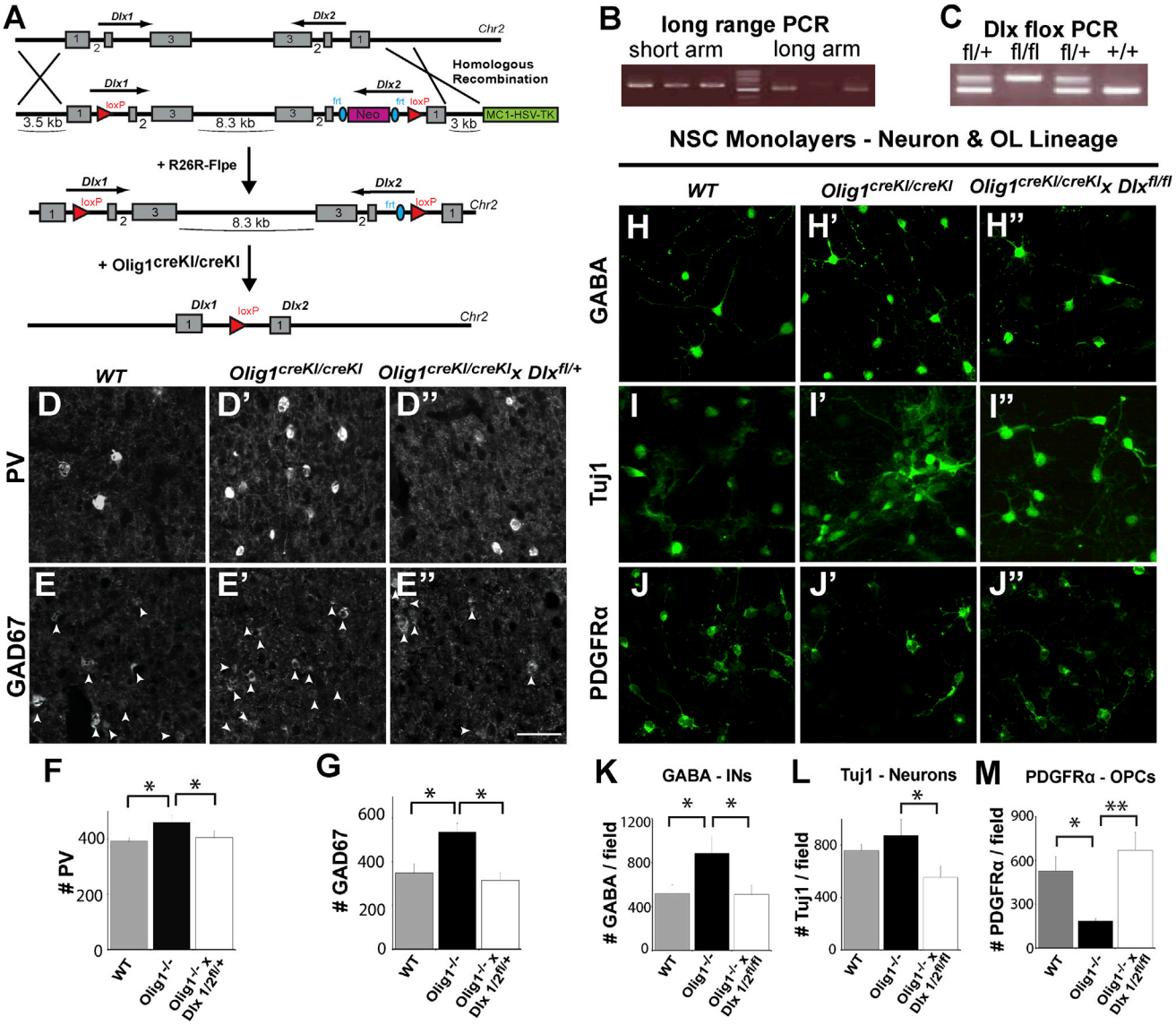

Figure 7. Increased Interneuron Production in *Olig1*-Null Animals Requires *Dlx1/2* Function In Vitro and In Vivo

(A) Schema illustrating the *Dlx1/2* flox targeting vector and strategy to knockout *Dlx1/2* within the *Olig1* lineage by generating *Dlx1/2*-floxed mice ($Dlx1/2^{fl/fl}$) and crossing them to *Olig1-cre* knockin mice ($Olig1^{cre(KI)/cre(KI)}$).

(B) Long-range PCR for the *Dlx1/2* floxed allele confirming successful homologous recombination and integration of the full targeting construct into founder (F1) mice.

(C) Representative image of PCR for the wild-type and *Dlx1/2* floxed alleles demonstrating successful derivation of floxed homozygous mice.

(D) Representative images of PV+ cells in cerebral cortex of P60 WT, $Olig1^{cre(KI)/cre(KI)}$, and $Olig1^{cre/cre}$ × $Dlx1/2^{fl/+}$ mice demonstrating that heterozygosity for *Dlx1/2* in the *Olig1* lineage is sufficient to rescue the increase in PV INs in *Olig1*-null mutants in vivo.

(E) Representative images of GAD67+ cells in cerebral cortex of P60 WT, $Olig1^{cre(KI)/cre(KI)}$, and $Olig1^{cre(KI)/cre(KI)}$ × $Dlx1/2^{fl/+}$ mice demonstrating that heterozygosity for *Dlx1/2* in the *Olig1* lineage is sufficient to rescue the increase in GAD67 INs in *Olig1*-null mutants in vivo.

(F and G) Quantification of the number of PV- and GAD67-expressing cells, respectively, in combined counts of motor and somatosensory cortex. (Mean ±SEM; n = 3; *p < 0.05; two-tailed unpaired Student's t test).

(H and I) Representative images (H) and (I) of GABA+ and Tuj1+ cells, respectively, generated by neural stem cell monolayer cultures derived from MGE of E14 WT, $Olig1^{cre/cre}$, and $Olig1^{cre(KI)/cre(KI)}$ × $Dlx1/2^{fl/fl}$ mice, demonstrating that genetic ablation of *Dlx1/2* in the *Olig1* lineage is sufficient to rescue the increase in GABAergic INs in *Olig1*-null mutants in vitro.

(J) Representative images of PDGFRa+ OPCs, demonstrating that *Dlx1/2* deletion in *Olig1* lineage cells rescues the diminution of the OL population observed in *Olig1* knockouts.

(K–M) Quantification of the number of GABA+, Tuj1+, and PDGFRa+ cells, respectively, in NSC monolayer cultures (mean ±SEM; n = 3 experiments; 2-slide wells per experiment; *p < 0.05; **p < 0.01, two-tailed unpaired Student's t test). In (E''), scale bar indicates 50 μm. See also Figure S7.

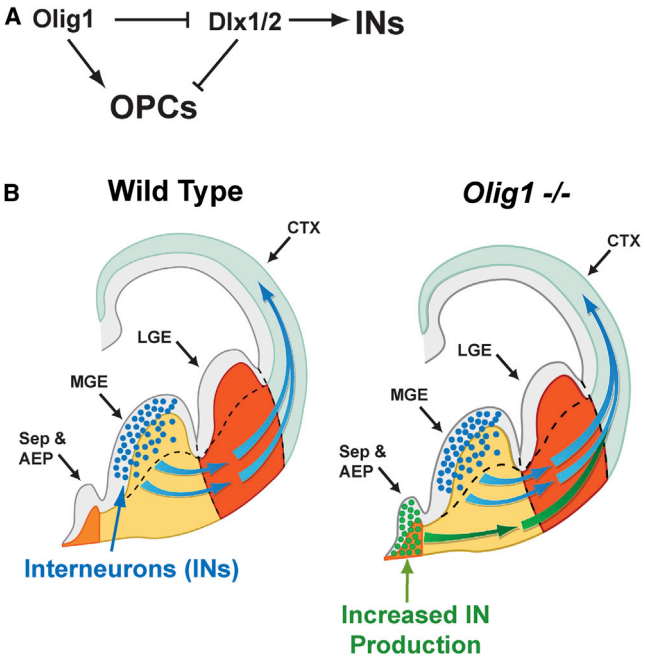

Figure 8. Model of the Mechanism of *Olig1* Function in the Ventral Telencephalon

(A) Schematic demonstrating genetic interaction between *Olig1* and *Dlx1/2* control specification of INs versus OLs. *Olig1* inhibits *Dlx1/2*, which are necessary for the production of interneurons and inhibit OL specification.

(B) *Olig1* inhibits production of INs from the vMGE, AEP, and septum.

and 7M). Taken together, these genetic findings support a model in which *Olig1* acts as an essential repressor of *Dlx1/2* to limit IN pool size and promote oligodendrogliogenesis (Figure 8A).

DISCUSSION

Recent studies indicate that the number of adult cortical INs is determined primarily at time of specification in the embryonic telencephalon, rather than through later neurotrophic competition, and developmental cell death (Southwell et al., 2012). Thus, limiting the number of cortical neurons produced during development is crucial. Here we show that *Olig1* represses *Dlx1/2* and IN production while preserving the potential to generate oligodendrocytes from common progenitors of the developing brain (Figure 8A).

Olig1 Functions as an Essential Repressor of IN Production in Mammalian Brain

We identified *Olig1* as a determinant of IN precursor pool size and IN numbers in the adult murine cortex. We observed an approximate 30% expansion of the total IN population, confined to PV+ and CR+ IN cell types, and a similar increase in PV/VGAT synapse density. This is consistent with previous findings that the maximum increase in density after transplantation of similar MGE progenitors into cortex is ~30% above normal (Baraban et al., 2009; Southwell et al., 2010, 2012). Based on these studies, it was unclear whether increased endogenous generation of INs in *Olig1*$^{-/-}$ mice would affect inhibitory activity on pyramidal cells. Indeed, we found that increased IN cortical density in *Olig1*-null mice did not induce changes in the number of inhibitory potentials on pyramidal cells in adult mouse cortex. This may reflect the increase in CR+ cells, which make inhibitory synapses on other INs (Caputi et al., 2009; Freund and Buzsáki, 1996; Gonchar and Burkhalter, 1999). It is also notable that expression of the postsynaptic scaffolding protein gephyrin is unaltered in *Olig1*-null mice. Gephyrin regulates the recruitment, stability, and clustering of GABA receptors at the postsynapse and is downregulated by increased inhibitory activity (Langosch et al., 1992; Poulopoulos et al., 2009; Prior et al., 1992; Saiepour et al., 2010; Tretter et al., 2008, 2012; Vlachos et al., 2012). These data suggest that the increased interneuron number in *Olig1*$^{-/-}$ mice might result in gephyrin-dependent postsynaptic compensation. We further demonstrated that *Olig1* is necessary to limit IN production in the CB and OB. Though numerous genes are required for IN specification and expansion, this is, to our knowledge, the first example of a transcription factor that represses cortical IN number.

Olig1 Regulates Neuron-Glial Fate Choice

The expansion of cortical IN number in *Olig1*$^{-/-}$ animals suggested a critical role in regulating embryonic neurogenesis. *Olig1* is not robustly expressed in forebrain until E12.5 (Lu et al., 2002), a time point that coincides with the onset of oligodendrocyte specification (He et al., 2001; Kessaris et al., 2006). Indeed, several lines of evidence support the hypothesis that *Olig1* regulates the neuron-glial switch. First, *Olig1* is coexpressed in Nkx2.1+ and Nestin+ multipotent radial glia. Second, we observed upregulation of pro-IN gene expression in ventral MGE and AEP of *Olig1*$^{-/-}$ animals (e.g., *Lhx6* and *Dlx1/2*), coupled with decreased OPC production in the ventral telencephalon. A surprising finding of the study was that the septum appears competent to produce INs in the absence of *Olig1* function (Figure 8B). Finally, *Olig1* limits production of PV+ and CR+ cells, which are derived late in embryogenesis from progenitor domains that produce both OLs and INs, but not NPY+ and SST+ cells, which are born prior to the onset of OL specification (Kessaris et al., 2006; Miyoshi et al., 2007; Taniguchi et al., 2013; Wonders et al., 2008). In support of broad roles for Olig1 in neuron-glial fate choice, we found enhanced neurogenesis in the CB and SVZ/OB. Taken together, our findings suggest that *Olig1* acts in regions of protracted neurogenesis to limit IN production and promote OPC specification in several brain regions.

Olig1 Regulates Cell Fate Choice in Multipotent Progenitors through Repressive Interactions with *Dlx1/2*

DNA binding and luciferase assays suggest that *Olig1* is a direct repressor of the *Dlx1/2* locus acting through E-boxes in the *I12b* intergenic enhancer (Ghanem et al., 2003, 2007; Park et al., 2004; Poitras et al., 2007). This model is supported by our mouse genetic experiments in which enhanced IN genesis in *Olig1*$^{-/-}$ is rescued by conditional removal of *Dlx1/2* from the *Olig1* expression domain. Together, our findings indicate *Olig1* is a repressor of *Dlx1/2*. Future studies will probe interactions of *Olig1* with

genes that control interneuron production in the CB and other brain regions.

Despite similar structural features, Olig1 and Olig2 are functionally distinct in many respects (Meijer et al., 2012), including expression pattern, posttranslational modification, cofactors, and transcriptional targets (Li et al., 2007; Li and Richardson, 2008; Lu et al., 2012). Our data show another unique role of Olig1 as an essential repressor of IN development. Prior studies show that forced *Olig1* overexpression results in ectopic OPC specification from neural progenitors (Kim et al., 2011; Lu et al., 2000, 2001; Maire et al., 2010). Although *Olig2* shows more robust expression than *Olig1* in the MGE and binds E-boxes in the *Dlx I12b* enhancer, this binding evidently is dispensable for IN genesis because we did not detect ectopic expression of *Dlx2* or *GAD67* in *Olig2*$^{-/-}$ animals despite upregulation of *Olig1* (Figure S4) (Petryniak et al., 2007, Furusho et al., 2006; Ono et al., 2008). Thus, *Olig1* shows a unique function in IN repression compared to *Olig2.*

Potential Roles for Olig1 in Human Brain Development and Disease Related to Interneuron Numbers and Inhibitory Tone

In the human fetal brain, OLIG1 proteins are expressed in primitive neuroepithelia that can give rise to INs (Jakovcevski and Zecevic, 2005), consistent with our findings. *OLIG1* and *OLIG2* are colocalized to human chromosome 21 in the Down syndrome (DS) critical region, and several studies report they are overexpressed in DS (Bhattacharyya et al., 2009; Chakrabarti et al., 2010). Certain behavioral and psychiatric disorders are associated with abnormal IN numbers, including Tourette's syndrome (Kalanithi et al., 2005; Kataoka et al., 2010) and schizophrenia (Hashimoto et al., 2003, 2008; Lewis et al., 2008). Our findings raise the possibility that *OLIG1* expression becomes dysregulated in certain pathological conditions.

Transplantation of progenitors for cortical INs deriving from the MGE can confer increased seizure threshold and alter plasticity (Baraban et al., 2009; Southwell et al., 2010). Recently, methods to derive human INs and OLs capable of transplantation, widespread migration, and functional integration into mammalian brain have been established (Maroof et al., 2013; Nicholas et al., 2013). IN transplants attenuate symptoms in rodent models of epilepsy (Baraban et al., 2009; Hunt et al., 2013), Parkinson's disease (Martínez-Cerdeño et al., 2010), and neuropathic pain (Bráz et al., 2012). Based on its properties to repress IN formation in cultured neural progenitors, reducing *Olig1* expression (e.g., siRNA) might provide a method to augment IN production for such potential therapeutic applications. Future studies will determine if increased IN number in *Olig1*$^{-/-}$ mice leads to differences in inhibitory tone during development, learning and memory tasks, and pathologies such as seizures.

EXPERIMENTAL PROCEDURES

Animals

All experimental procedures were approved by the Institutional Animal Care and Use Committee and Laboratory Animal Resource Center at the University of California San Francisco (UCSF). Mouse colonies were maintained at UCSF in accordance with National Institutes of Health and UCSF guidelines. The *Olig1*$^{cre/cre}$ (Lu et al., 2002) and *Caggs-EGFP* (Nakamura et al., 2006) reporter mice have been previously described. The Dlx1/2$^{fl/fl}$ mice were generated as described in the Supplemental Experimental Procedures.

ISH and IHC

ISH and IHC were performed using standard protocols. Table S1 lists details of antibodies, and protocols for ISH, IHC, and BrdU labeling are provided in the Supplemental Experimental Procedures.

rtPCR

RNA was isolated (Trizol extraction followed by RNeasy; QIAGEN) from MGE plus septum, reversed transcribed, and assayed for gene expression by SYBR-Green technology on a Lightcycler 480 (Roche). Primer sequences and details of analytical methods and statistics can be found in the Supplemental Experimental Procedures.

Neural Progenitor Cultures

Neurosphere and neural stem cell monolayer cultures were derived from E14 ventral telencephalon or P3 SVZ by standard methods (Ahlenius and Kokaia, 2010). Details of culture preparations and western blot analysis of these cultures are provided in the Supplemental Experimental Procedures.

Microscopy, Cell Counting, and Statistical Analyses

Cell populations were quantified in vivo from micrographs of identical field size of anatomically matched regions of somatosensory, motor cortex, and corpus callosum. In vitro cell populations cultured in 8-well culture slides were sampled at defined points within each slide well using a Nikon 80i microscope equipped with a motorized stage. Cell counts were conducted by a researcher blinded to genotype using ImageJ and Nikon Elements software. Statistical significance was determined using unpaired, two-tailed Student's t tests.

DNA Binding and Luciferase Assays

These methods are detailed in the Supplemental Experimental Procedures.

SUPPLEMENTAL INFORMATION

Supplemental Information includes seven figures, one table, and Supplemental Experimental Procedures and can be found with this article online at http://dx.doi.org/10.1016/j.neuron.2013.11.024.

ACKNOWLEDGMENTS

We are grateful to Michael Wong and Sandra Chang for expert technical help. J. S. acknowledges support from training grant T32 GM007449-36 from the NIGMS and the Ruth Kirschstein NRSA fellowship F31 NS076254-03 from the NINDS. G.P. and H.N acknowledge postdoctoral fellowship support from the European Leukodystrophy Association. This work has been supported by grants to C.D.S. (NS047572) and D.H.R. (NS040511) from the NINDS, to J.L.R.R. (MH049428) from NIMH, and to S.C.B (R01-NS-048528) from NINDS. D.H.R. is an Howard Hughes Medical Institute Investigator.

Accepted: November 4, 2013
Published: February 5, 2014

REFERENCES

Ahlenius, H., and Kokaia, Z. (2010). Isolation and generation of neurosphere cultures from embryonic and adult mouse brain. Methods Mol. Biol. *633*, 241–252.

Alonso, J.M., and Swadlow, H.A. (2005). Thalamocortical specificity and the synthesis of sensory cortical receptive fields. J. Neurophysiol. *94*, 26–32.

Alvarez-Buylla, A., Seri, B., and Doetsch, F. (2002). Identification of neural stem cells in the adult vertebrate brain. Brain Res. Bull. *57*, 751–758.

Alvarez-Dolado, M., Calcagnotto, M.E., Karkar, K.M., Southwell, D.G., Jones-Davis, D.M., Estrada, R.C., Rubenstein, J.L., Alvarez-Buylla, A., and Baraban,

S.C. (2006). Cortical inhibition modified by embryonic neural precursors grafted into the postnatal brain. J. Neurosci. *26*, 7380–7389.

Anderson, S.A., Eisenstat, D.D., Shi, L., and Rubenstein, J.L. (1997). Interneuron migration from basal forebrain to neocortex: dependence on Dlx genes. Science *278*, 474–476.

Arnett, H.A., Fancy, S.P., Alberta, J.A., Zhao, C., Plant, S.R., Kaing, S., Raine, C.S., Rowitch, D.H., Franklin, R.J., and Stiles, C.D. (2004). bHLH transcription factor Olig1 is required to repair demyelinated lesions in the CNS. Science *306*, 2111–2115.

Baraban, S.C., Southwell, D.G., Estrada, R.C., Jones, D.L., Sebe, J.Y., Alfaro-Cervello, C., García-Verdugo, J.M., Rubenstein, J.L., and Alvarez-Buylla, A. (2009). Reduction of seizures by transplantation of cortical GABAergic interneuron precursors into Kv1.1 mutant mice. Proc. Natl. Acad. Sci. USA *106*, 15472–15477.

Ben-Ari, Y. (2006). Seizures beget seizures: the quest for GABA as a key player. Crit. Rev. Neurobiol. *18*, 135–144.

Bhattacharyya, A., McMillan, E., Chen, S.I., Wallace, K., and Svendsen, C.N. (2009). A critical period in cortical interneuron neurogenesis in down syndrome revealed by human neural progenitor cells. Dev. Neurosci. *31*, 497–510.

Bragina, L., Candiracci, C., Barbaresi, P., Giovedì, S., Benfenati, F., and Conti, F. (2007). Heterogeneity of glutamatergic and GABAergic release machinery in cerebral cortex. Neuroscience *146*, 1829–1840.

Bráz, J.M., Sharif-Naeini, R., Vogt, D., Kriegstein, A., Alvarez-Buylla, A., Rubenstein, J.L., and Basbaum, A.I. (2012). Forebrain GABAergic neuron precursors integrate into adult spinal cord and reduce injury-induced neuropathic pain. Neuron *74*, 663–675.

Butt, S.J., Fuccillo, M., Nery, S., Noctor, S., Kriegstein, A., Corbin, J.G., and Fishell, G. (2005). The temporal and spatial origins of cortical interneurons predict their physiological subtype. Neuron *48*, 591–604.

Butt, S.J., Sousa, V.H., Fuccillo, M.V., Hjerling-Leffler, J., Miyoshi, G., Kimura, S., and Fishell, G. (2008). The requirement of Nkx2-1 in the temporal specification of cortical interneuron subtypes. Neuron *59*, 722–732.

Caputi, A., Rozov, A., Blatow, M., and Monyer, H. (2009). Two calretinin-positive GABAergic cell types in layer 2/3 of the mouse neocortex provide different forms of inhibition. Cereb. Cortex *19*, 1345–1359.

Chakrabarti, L., Best, T.K., Cramer, N.P., Carney, R.S., Isaac, J.T., Galdzicki, Z., and Haydar, T.F. (2010). Olig1 and Olig2 triplication causes developmental brain defects in Down syndrome. Nat. Neurosci. *13*, 927–934.

Cobos, I., Calcagnotto, M.E., Vilaythong, A.J., Thwin, M.T., Noebels, J.L., Baraban, S.C., and Rubenstein, J.L. (2005). Mice lacking Dlx1 show subtype-specific loss of interneurons, reduced inhibition and epilepsy. Nat. Neurosci. *8*, 1059–1068.

Corbin, J.G., Nery, S., and Fishell, G. (2001). Telencephalic cells take a tangent: non-radial migration in the mammalian forebrain. Nat. Neurosci. *4* (*Suppl*), 1177–1182.

Elias, L.A., Potter, G.B., and Kriegstein, A.R. (2008). A time and a place for nkx2-1 in interneuron specification and migration. Neuron *59*, 679–682.

Freund, T.F., and Buzsáki, G. (1996). Interneurons of the hippocampus. Hippocampus *6*, 347–470.

Furusho, M., Ono, K., Takebayashi, H., Masahira, N., Kagawa, T., Ikeda, K., and Ikenaka, K. (2006). Involvement of the Olig2 transcription factor in cholinergic neuron development of the basal forebrain. Dev. Biol. *293*, 348–357.

Ghanem, N., Jarinova, O., Amores, A., Long, Q., Hatch, G., Park, B.K., Rubenstein, J.L., and Ekker, M. (2003). Regulatory roles of conserved intergenic domains in vertebrate Dlx bigene clusters. Genome Res. *13*, 533–543.

Ghanem, N., Yu, M., Long, J., Hatch, G., Rubenstein, J.L., and Ekker, M. (2007). Distinct cis-regulatory elements from the Dlx1/Dlx2 locus mark different progenitor cell populations in the ganglionic eminences and different subtypes of adult cortical interneurons. J. Neurosci. *27*, 5012–5022.

Goldman, J.E., Zerlin, M., Newman, S., Zhang, L., and Gensert, J. (1997). Fate determination and migration of progenitors in the postnatal mammalian CNS. Dev. Neurosci. *19*, 42–48.

Gonchar, Y., and Burkhalter, A. (1999). Connectivity of GABAergic calretinin-immunoreactive neurons in rat primary visual cortex. Cereb. Cortex *9*, 683–696.

Han, S., Tai, C., Westenbroek, R.E., Yu, F.H., Cheah, C.S., Potter, G.B., Rubenstein, J.L., Scheuer, T., de la Iglesia, H.O., and Catterall, W.A. (2012). Autistic-like behaviour in Scn1a+/- mice and rescue by enhanced GABA-mediated neurotransmission. Nature *489*, 385–390.

Hashimoto, T., Volk, D.W., Eggan, S.M., Mirnics, K., Pierri, J.N., Sun, Z., Sampson, A.R., and Lewis, D.A. (2003). Gene expression deficits in a subclass of GABA neurons in the prefrontal cortex of subjects with schizophrenia. J. Neurosci. *23*, 6315–6326.

Hashimoto, T., Arion, D., Unger, T., Maldonado-Avilés, J.G., Morris, H.M., Volk, D.W., Mirnics, K., and Lewis, D.A. (2008). Alterations in GABA-related transcriptome in the dorsolateral prefrontal cortex of subjects with schizophrenia. Mol. Psychiatry *13*, 147–161.

He, W., Ingraham, C., Rising, L., Goderie, S., and Temple, S. (2001). Multipotent stem cells from the mouse basal forebrain contribute GABAergic neurons and oligodendrocytes to the cerebral cortex during embryogenesis. J. Neurosci. *21*, 8854–8862.

Hunt, R.F., Girskis, K.M., Rubenstein, J.L., Alvarez-Buylla, A., and Baraban, S.C. (2013). GABA progenitors grafted into the adult epileptic brain control seizures and abnormal behavior. Nat. Neurosci. *16*, 692–697.

Jakovcevski, I., and Zecevic, N. (2005). Olig transcription factors are expressed in oligodendrocyte and neuronal cells in human fetal CNS. J. Neurosci. *25*, 10064–10073.

Kalanithi, P.S., Zheng, W., Kataoka, Y., DiFiglia, M., Grantz, H., Saper, C.B., Schwartz, M.L., Leckman, J.F., and Vaccarino, F.M. (2005). Altered parvalbumin-positive neuron distribution in basal ganglia of individuals with Tourette syndrome. Proc. Natl. Acad. Sci. USA *102*, 13307–13312.

Kataoka, Y., Kalanithi, P.S., Grantz, H., Schwartz, M.L., Saper, C., Leckman, J.F., and Vaccarino, F.M. (2010). Decreased number of parvalbumin and cholinergic interneurons in the striatum of individuals with Tourette syndrome. J. Comp. Neurol. *518*, 277–291.

Kehrer, C., Maziashvili, N., Dugladze, T., and Gloveli, T. (2008). Altered Excitatory-Inhibitory Balance in the NMDA-Hypofunction Model of Schizophrenia. Front. Mol. Neurosci. *1*, 6.

Kessaris, N., Fogarty, M., Iannarelli, P., Grist, M., Wegner, M., and Richardson, W.D. (2006). Competing waves of oligodendrocytes in the forebrain and postnatal elimination of an embryonic lineage. Nat. Neurosci. *9*, 173–179.

Kim, H.M., Hwang, D.H., Choi, J.Y., Park, C.H., Suh-Kim, H., Kim, S.U., and Kim, B.G. (2011). Differential and cooperative actions of Olig1 and Olig2 transcription factors on immature proliferating cells after contusive spinal cord injury. Glia *59*, 1094–1106.

Langosch, D., Hoch, W., and Betz, H. (1992). The 93 kDa protein gephyrin and tubulin associated with the inhibitory glycine receptor are phosphorylated by an endogenous protein kinase. FEBS Lett *298*, 113–117.

Lee, S.K., Lee, B., Ruiz, E.C., and Pfaff, S.L. (2005). Olig2 and Ngn2 function in opposition to modulate gene expression in motor neuron progenitor cells. Genes Dev. *19*, 282–294.

Lehmann, K., Steinecke, A., and Bolz, J. (2012). GABA through the ages: regulation of cortical function and plasticity by inhibitory interneurons. Neural Plast. *2012*, 892784.

Lewis, D.A., Hashimoto, T., and Volk, D.W. (2005). Cortical inhibitory neurons and schizophrenia. Nat. Rev. Neurosci. *6*, 312–324.

Lewis, D.A., Hashimoto, T., and Morris, H.M. (2008). Cell and receptor type-specific alterations in markers of GABA neurotransmission in the prefrontal cortex of subjects with schizophrenia. Neurotox. Res. *14*, 237–248.

Li, H., and Richardson, W.D. (2008). The evolution of Olig genes and their roles in myelination. Neuron Glia Biol. *4*, 129–135.

Li, H., Lu, Y., Smith, H.K., and Richardson, W.D. (2007). Olig1 and Sox10 interact synergistically to drive myelin basic protein transcription in oligodendrocytes. J. Neurosci. *27*, 14375–14382.

Llinás, R., Urbano, F.J., Leznik, E., Ramírez, R.R., and van Marle, H.J. (2005). Rhythmic and dysrhythmic thalamocortical dynamics: GABA systems and the edge effect. Trends Neurosci. *28*, 325–333.

Long, J.E., Garel, S., Alvarez-Dolado, M., Yoshikawa, K., Osumi, N., Alvarez-Buylla, A., and Rubenstein, J.L. (2007). Dlx-dependent and -independent regulation of olfactory bulb interneuron differentiation. J. Neurosci. *27*, 3230–3243.

Lu, Q.R., Yuk, D., Alberta, J.A., Zhu, Z., Pawlitzky, I., Chan, J., McMahon, A.P., Stiles, C.D., and Rowitch, D.H. (2000). Sonic hedgehog—regulated oligodendrocyte lineage genes encoding bHLH proteins in the mammalian central nervous system. Neuron *25*, 317–329.

Lu, Q.R., Cai, L., Rowitch, D., Cepko, C.L., and Stiles, C.D. (2001). Ectopic expression of Olig1 promotes oligodendrocyte formation and reduces neuronal survival in developing mouse cortex. Nat. Neurosci. *4*, 973–974.

Lu, Q.R., Sun, T., Zhu, Z., Ma, N., Garcia, M., Stiles, C.D., and Rowitch, D.H. (2002). Common developmental requirement for Olig function indicates a motor neuron/oligodendrocyte connection. Cell *109*, 75–86.

Lu, J., Lian, G., Zhou, H., Esposito, G., Steardo, L., Delli-Bovi, L.C., Hecht, J.L., Lu, Q.R., and Sheen, V. (2012). OLIG2 over-expression impairs proliferation of human Down syndrome neural progenitors. Hum. Mol. Genet. *21*, 2330–2340.

Maire, C.L., Wegener, A., Kerninon, C., and Nait Oumesmar, B. (2010). Gain-of-function of Olig transcription factors enhances oligodendrogenesis and myelination. Stem Cells *28*, 1611–1622.

Maricich, S.M., and Herrup, K. (1999). Pax-2 expression defines a subset of GABAergic interneurons and their precursors in the developing murine cerebellum. J. Neurobiol. *41*, 281–294.

Marín, O. (2012). Brain development: The neuron family tree remodelled. Nature *490*, 185–186.

Maroof, A.M., Keros, S., Tyson, J.A., Ying, S.W., Ganat, Y.M., Merkle, F.T., Liu, B., Goulburn, A., Stanley, E.G., Elefanty, A.G., et al. (2013). Directed differentiation and functional maturation of cortical interneurons from human embryonic stem cells. Cell Stem Cell *12*, 559–572.

Martínez-Cerdeño, V., Noctor, S.C., Espinosa, A., Ariza, J., Parker, P., Orasji, S., Daadi, M.M., Bankiewicz, K., Alvarez-Buylla, A., and Kriegstein, A.R. (2010). Embryonic MGE precursor cells grafted into adult rat striatum integrate and ameliorate motor symptoms in 6-OHDA-lesioned rats. Cell Stem Cell *6*, 238–250.

Meijer, D.H., Kane, M.F., Mehta, S., Liu, H., Harrington, E., Taylor, C.M., Stiles, C.D., and Rowitch, D.H. (2012). Separated at birth? The functional and molecular divergence of OLIG1 and OLIG2. Nat. Rev. Neurosci. *13*, 819–831.

Menn, B., Garcia-Verdugo, J.M., Yaschine, C., Gonzalez-Perez, O., Rowitch, D., and Alvarez-Buylla, A. (2006). Origin of oligodendrocytes in the subventricular zone of the adult brain. J. Neurosci. *26*, 7907–7918.

Miyoshi, G., Butt, S.J., Takebayashi, H., and Fishell, G. (2007). Physiologically distinct temporal cohorts of cortical interneurons arise from telencephalic Olig2-expressing precursors. J. Neurosci. *27*, 7786–7798.

Mukhopadhyay, A., McGuire, T., Peng, C.Y., and Kessler, J.A. (2009). Differential effects of BMP signaling on parvalbumin and somatostatin interneuron differentiation. Development *136*, 2633–2642.

Nakamura, T., Colbert, M.C., and Robbins, J. (2006). Neural crest cells retain multipotential characteristics in the developing valves and label the cardiac conduction system. Circ. Res. *98*, 1547–1554.

Nicholas, C.R., Chen, J., Tang, Y., Southwell, D.G., Chalmers, N., Vogt, D., Arnold, C.M., Chen, Y.J., Stanley, E.G., Elefanty, A.G., et al. (2013). Functional maturation of hPSC-derived forebrain interneurons requires an extended timeline and mimics human neural development. Cell Stem Cell *12*, 573–586.

Novitch, B.G., Chen, A.I., and Jessell, T.M. (2001). Coordinate regulation of motor neuron subtype identity and pan-neuronal properties by the bHLH repressor Olig2. Neuron *31*, 773–789.

Ono, K., Takebayashi, H., Ikeda, K., Furusho, M., Nishizawa, T., Watanabe, K., and Ikenaka, K. (2008). Regional- and temporal-dependent changes in the differentiation of Olig2 progenitors in the forebrain, and the impact on astrocyte development in the dorsal pallium. Dev. Biol. *320*, 456–468.

Park, B.K., Sperber, S.M., Choudhury, A., Ghanem, N., Hatch, G.T., Sharpe, P.T., Thomas, B.L., and Ekker, M. (2004). Intergenic enhancers with distinct activities regulate Dlx gene expression in the mesenchyme of the branchial arches. Dev. Biol. *268*, 532–545.

Petryniak, M.A., Potter, G.B., Rowitch, D.H., and Rubenstein, J.L. (2007). Dlx1 and Dlx2 control neuronal versus oligodendroglial cell fate acquisition in the developing forebrain. Neuron *55*, 417–433.

Poitras, L., Ghanem, N., Hatch, G., and Ekker, M. (2007). The proneural determinant MASH1 regulates forebrain Dlx1/2 expression through the I12b intergenic enhancer. Development *134*, 1755–1765.

Potter, G.B., Petryniak, M.A., Shevchenko, E., McKinsey, G.L., Ekker, M., and Rubenstein, J.L. (2009). Generation of Cre-transgenic mice using Dlx1/Dlx2 enhancers and their characterization in GABAergic interneurons. Mol. Cell. Neurosci. *40*, 167–186.

Poulopoulos, A., Aramuni, G., Meyer, G., Soykan, T., Hoon, M., Papadopoulos, T., Zhang, M., Paarmann, I., Fuchs, C., Harvey, K., et al. (2009). Neuroligin 2 drives postsynaptic assembly at perisomatic inhibitory synapses through gephyrin and collybistin. Neuron *63*, 628–642.

Pozo, K., and Goda, Y. (2010). Unraveling mechanisms of homeostatic synaptic plasticity. Neuron *66*, 337–351.

Prior, P., Schmitt, B., Grenningloh, G., Pribilla, I., Multhaup, G., Beyreuther, K., Maulet, Y., Werner, P., Langosch, D., Kirsch, J., et al. (1992). Primary structure and alternative splice variants of gephyrin, a putative glycine receptor-tubulin linker protein. Neuron *8*, 1161–1170.

Rossignol, E. (2011). Genetics and function of neocortical GABAergic interneurons in neurodevelopmental disorders. Neural Plast. *2011*, 649325.

Rubenstein, J.L. (2010). Three hypotheses for developmental defects that may underlie some forms of autism spectrum disorder. Curr. Opin. Neurol. *23*, 118–123.

Rubenstein, J.L., and Merzenich, M.M. (2003). Model of autism: increased ratio of excitation/inhibition in key neural systems. Genes Brain Behav. *2*, 255–267.

Rubin, A.N., Alfonsi, F., Humphreys, M.P., Choi, C.K., Rocha, S.F., and Kessaris, N. (2010). The germinal zones of the basal ganglia but not the septum generate GABAergic interneurons for the cortex. J. Neurosci. *30*, 12050–12062.

Saiepour, L., Fuchs, C., Patrizi, A., Sassoè-Pognetto, M., Harvey, R.J., and Harvey, K. (2010). Complex role of collybistin and gephyrin in GABAA receptor clustering. J. Biol. Chem. *285*, 29623–29631.

Samanta, J., Burke, G.M., McGuire, T., Pisarek, A.J., Mukhopadhyay, A., Mishina, Y., and Kessler, J.A. (2007). BMPR1a signaling determines numbers of oligodendrocytes and calbindin-expressing interneurons in the cortex. J. Neurosci. *27*, 7397–7407.

Schiller, P.H., and Tehovnik, E.J. (2005). Neural mechanisms underlying target selection with saccadic eye movements. Prog. Brain Res. *149*, 157–171.

Schüller, U., Kho, A.T., Zhao, Q., Ma, Q., and Rowitch, D.H. (2006). Cerebellar 'transcriptome' reveals cell-type and stage-specific expression during postnatal development and tumorigenesis. Mol. Cell. Neurosci. *33*, 247–259.

Silbereis, J., Cheng, E., Ganat, Y.M., Ment, L.R., and Vaccarino, F.M. (2009). Precursors with glial fibrillary acidic protein promoter activity transiently generate GABA interneurons in the postnatal cerebellum. Stem Cells *27*, 1152–1163.

Southwell, D.G., Froemke, R.C., Alvarez-Buylla, A., Stryker, M.P., and Gandhi, S.P. (2010). Cortical plasticity induced by inhibitory neuron transplantation. Science *327*, 1145–1148.

Southwell, D.G., Paredes, M.F., Galvao, R.P., Jones, D.L., Froemke, R.C., Sebe, J.Y., Alfaro-Cervello, C., Tang, Y., Garcia-Verdugo, J.M., Rubenstein, J.L., et al. (2012). Intrinsically determined cell death of developing cortical interneurons. Nature *491*, 109–113.

Sun, T., Dong, H., Wu, L., Kane, M., Rowitch, D.H., and Stiles, C.D. (2003). Cross-repressive interaction of the Olig2 and Nkx2.2 transcription factors in developing neural tube associated with formation of a specific physical complex. J. Neurosci. *23*, 9547–9556.

Taglialatela, P., Soria, J.M., Caironi, V., Moiana, A., and Bertuzzi, S. (2004). Compromised generation of GABAergic interneurons in the brains of Vax1-/- mice. Development *131*, 4239–4249.

Taniguchi, H., Lu, J., and Huang, Z.J. (2013). The spatial and temporal origin of chandelier cells in mouse neocortex. Science *339*, 70–74.

Tretter, V., Jacob, T.C., Mukherjee, J., Fritschy, J.M., Pangalos, M.N., and Moss, S.J. (2008). The clustering of GABA(A) receptor subtypes at inhibitory synapses is facilitated via the direct binding of receptor alpha 2 subunits to gephyrin. J. Neurosci. *28*, 1356–1365.

Tretter, V., Mukherjee, J., Maric, H.M., Schindelin, H., Sieghart, W., and Moss, S.J. (2012). Gephyrin, the enigmatic organizer at GABAergic synapses. Front. Cell. Neurosci. *6*, http://dx.doi.org/10.3389/fncel.2012.00023.

Turrigiano, G. (2011). Too many cooks? Intrinsic and synaptic homeostatic mechanisms in cortical circuit refinement. Annu. Rev. Neurosci. *34*, 89–103.

Vlachos, A., Reddy-Alla, S., Papadopoulos, T., Deller, T., and Betz, H. (2012). Homeostatic regulation of gephyrin scaffolds and synaptic strength at mature hippocampal GABAergic postsynapses. Cereb. Cortex *23*, 2700–2711.

Waclaw, R.R., Allen, Z.J., 2nd, Bell, S.M., Erdélyi, F., Szabó, G., Potter, S.S., and Campbell, K. (2006). The zinc finger transcription factor Sp8 regulates the generation and diversity of olfactory bulb interneurons. Neuron *49*, 503–516.

Wonders, C.P., and Anderson, S.A. (2006). The origin and specification of cortical interneurons. Nat. Rev. Neurosci. *7*, 687–696.

Wonders, C.P., Taylor, L., Welagen, J., Mbata, I.C., Xiang, J.Z., and Anderson, S.A. (2008). A spatial bias for the origins of interneuron subgroups within the medial ganglionic eminence. Dev. Biol. *314*, 127–136.

Xin, M., Yue, T., Ma, Z., Wu, F.F., Gow, A., and Lu, Q.R. (2005). Myelinogenesis and axonal recognition by oligodendrocytes in brain are uncoupled in Olig1-null mice. J. Neurosci. *25*, 1354–1365.

Yizhar, O., Fenno, L.E., Prigge, M., Schneider, F., Davidson, T.J., O'Shea, D.J., Sohal, V.S., Goshen, I., Finkelstein, J., Paz, J.T., et al. (2011). Neocortical excitation/inhibition balance in information processing and social dysfunction. Nature *477*, 171–178.

Zhang, L., and Goldman, J.E. (1996). Generation of cerebellar interneurons from dividing progenitors in white matter. Neuron *16*, 47–54.